

^{233}U mass yield measurements around and within the symmetry region with the ILL Lohengrin spectrometer

A. Chebboubi¹, G. Kessedjian¹, C. Sage^{1,a}, D. Bernard², A. Blanc³, H. Faust³, U. Köster³, O. Litaize², P. Mutti³, and O. Serot²

¹LPSC, Université Grenoble-Alpes, CNRS/IN2P3, F-38026 Grenoble Cedex, France

²CEA, DEN, DER, SPRC, Cadarache, Physics Studies Laboratory, F-13108 Saint-Paul-lès-Durance, France

³Institut Laue-Langevin, F-38042 Grenoble Cedex 9, France

Abstract. The study of fission yields has a major impact on the characterization and understanding of the fission process and is mandatory for reactor applications. The LPSC in collaboration with ILL and CEA has developed a measurement program on fission fragment distributions at the Lohengrin spectrometer of the ILL, with a special focus on the masses constituting the heavy peak. We will present in this paper our measurement of the very low fission yields in the symmetry mass region and the heavy mass wing of the distribution for ^{233}U thermal neutron induced fission. The difficulty due to the strong contamination by other masses with much higher yields will be addressed in the form of a new analysis method featuring the required contaminant correction. The apparition of structures in the kinetic energy distributions and possible interpretations will be discussed, such as a possible evidence of fission modes.

1 Introduction

The accurate knowledge of the fission data in the actinide region is important for studies of innovative nuclear reactor concepts. Today, in the framework of nuclear data evaluation, fission models are necessary to increase the consistency and the precision of the libraries. For instance, post neutron fission yields are actually needed in the current and innovative fuel cycles for the calculation of the inventory and the radiotoxicity of the spent fuel, and the estimation of the residual power after shutdown.

Moreover, fission yield measurements supply experimental data to put constraints on fission models and improve their predictive power. In this context, since 2007, various experiments from our collaboration have been performed to investigate fission yields at the Lohengrin spectrometer of the ILL with a special focus on the heavy mass and symmetry region, where can be found an inconsistency between models or evaluations and the scarce experimental data.

Recent measurements from [1, 2] of ^{233}U fission yields in the heavy region with the Lohengrin spectrometer showed an important discrepancy near the symmetry region when compared to evaluations. This is shown in Fig. 1 where these measurements are displayed with the JEFF-3.1.1 evaluations [3]. Firstly, our work presented here constitutes a deep investigation around and within the symmetry region to explain this disagreement and get accurate fission yields, which is a key element

^ae-mail: sage@lpsc.in2p3.fr

to ensure the self-normalisation of our data [1, 2]. A second important goal of our work here is to take this opportunity to study the structures in the fission fragment kinetic energy distributions and use symmetric fission as a laboratory to test fission models.

2 Experimental setup: the Lohengrin spectrometer

The Lohengrin mass spectrometer [4] is a nuclear physics instrument from the ILL research reactor facility which allows to study fragment distributions from thermal neutron induced fission with a very good resolution. A fissile actinide target is placed close to the reactor core, in a thermal neutron flux reaching 5×10^{14} neutron.cm⁻².s⁻¹.

Fission fragments emerge from the target with an ionic charge distributed around an average ionic charge state of about 21. Those fragments that are emitted along the beam tube axis undergo a horizontal deflection in a magnetic field, directly followed by a vertical deflection in an electric field. These combined fields separate ions according to their A/q and E/q ratios, with A , q and E the mass, ionic charge state and kinetic energy of the ions respectively.

At the spectrometer exit, different detection systems can be installed, such as an ionisation chamber for mass yield measurements, or Ge clovers that are used with an additional magnet whose aim is to focus the ion beam. A schematic view of the spectrometer is shown in Fig 1.

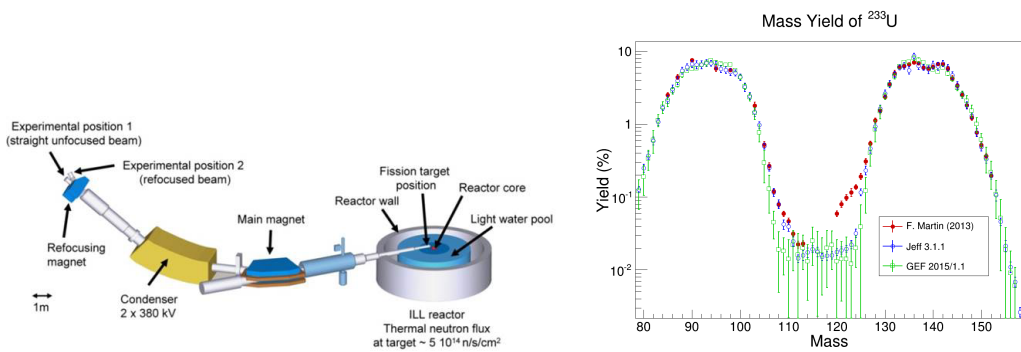


Figure 1. Schematic overview of the Lohengrin spectrometer at the ILL (left). $^{233}\text{U}(n_{th}, f)$ fission yields from F. Martin *et al.*[2] (right).

3 Yield measurements around and within the symmetry region

3.1 Absolute mass yields in the heavy region

High yields in the heavy region are obtained after an integration over the kinetic energy and the ionic charge distributions of the count rates measured with the ionisation chamber. A new measurement method and consequent analysis path have been developed and are detailed in Ref [1, 2]. Among the special features of this method are the self-normalisation of our data and the calculation of the experimental covariance matrices. Provided that all the heavy mass rates are measured, it is possible to self-normalise the data by defining to 100 % the sum of the whole heavy peak yields. As a consequence, these new measurements are independent from another experiment or assessment and may be compared directly with the existing data and evaluations. The results for $^{233}\text{U}(n_{th}, f)$ are shown in

Fig. 1 and present a clear difference of the yields on the way down to the symmetry region. The goal of this work is the complete analysis of the ionic charge and the kinetic energy distributions which present structures that had not been seen in past works [5].

3.2 Contamination highlighting

In the descent to the symmetry region ($A < 130$), a second component appears at low kinetic energy. We previously observed this component to be sensitive to the pressure of the spectrometer. The evolution of this effect with pressure is shown in Fig. 2. This phenomenon is explained as a consequence of ionic charge exchange between the fission fragment and the residual gas of the Lohengrin vacuum. If we consider that the main magnet selected the fragments with mass A_0 and A_1 with the condition $\frac{A_0 v_0}{q_0} = \frac{A_1 v_1}{q_1}$ followed by a charge change for the second fragment $q_1 \rightarrow q'_1$, then the condenser will select the kinetic energies following the equation :

$$\frac{E_0}{q_0} = \frac{E_1}{q'_1} \Leftrightarrow \frac{A_0 v_0^2}{q_0} = \frac{A_1 v_1^2}{q'_1} \tag{1}$$

Since this contaminant will appear at the same energy in the ionisation chamber, we get the following condition on the charge : $E_1 = E_0 \Leftrightarrow q'_1 = q_0$. Consequently the contaminant mass follows the relation $A_1 = \left(\frac{v_0}{v_1}\right)^2 A_0$. If we compare to the initial condition from the magnet we get the final relation for the contaminant :

$$A_1 = \left(\frac{q_1}{q_0}\right)^2 A_0 \tag{2}$$

This hypothesis was investigated with the building of an indicator based on equation 2. Fig. 2 shows the indicator results for mass 124. The masses with discrepant count rates out of the distribution shaped by the other ones are typically the masses with the highest contamination indicator values. This indicator was validated by gamma spectrometry, where the presence of the expected contaminant was proven.

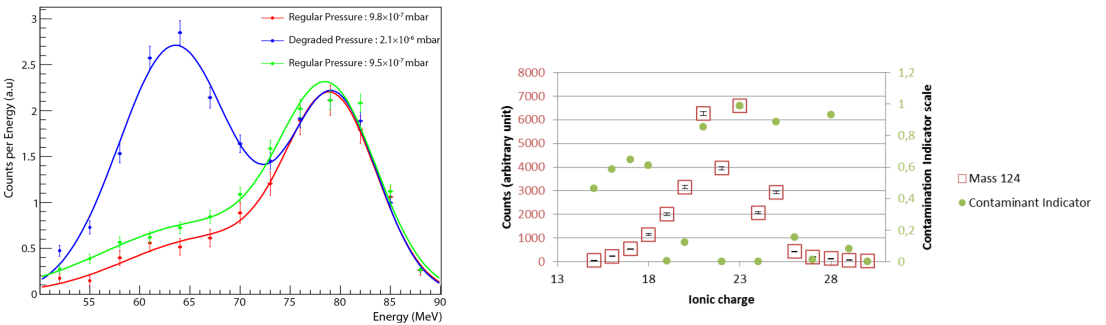


Figure 2. Influence of the condenser pressure on the kinetic energy distribution (left). Contamination indicator for the mass 124 as a function of ionic charge (right).

3.3 Analysis method for the contamination correction

The contaminant subtraction was achieved on the kinetic energy distributions $P(E_k)$ following equation 3.

$$P(E_k)^{sym} = P(E_k)^{meas} - \sum_{cont} P_{qq'} \times P_{ind} \times \frac{Y(A_{cont})}{Y(A_{sym})} \times P(E_k)^{cont} \quad (3)$$

where $P_{qq'}$ represents the measured charge changing probabilities using γ spectroscopy. These probabilities have the same order of magnitude for several nuclei. In the following, it will be supposed identical for all isotopes : $P_{q \rightarrow q+1} \sim 0.02$, $P_{q \rightarrow q+2} \sim 0.0013$ and $P_{q \rightarrow q-1} \sim 0.02$.

P_{ind} is linked to the presence of the contaminant in the ionisation chamber and is based on the indicator derived from equation 2. The correction factor is weighted by the yield ratio of the contaminant mass (with a higher yield) over the measured symmetry mass, multiplied by the kinetic energy distribution of the contaminant mass $P(E_k)^{cont}$.

Figure 3 shows the results of such a correction for the kinetic energy distributions of masses 116 and 118. We can notice that the presence of two components in the distribution remains after the correction, and this is the case for all masses around and within the symmetry region. Moreover, even if we consider $P_{qq'}$ as free parameters, it is not possible to fully suppress the low component.

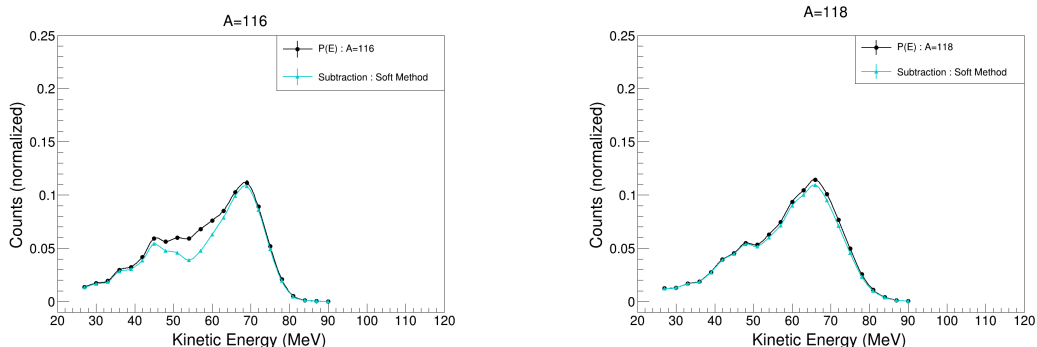


Figure 3. Kinetic energy distributions before (black) and after (blue) contaminant correction for masses 116 (left) and 118 (right).

4 Preliminary results and discussion

Figure 4 shows the preliminary results for our symmetry yield measurements. The yields are shown in the case of no correction (black dots), corrected (red dots), but also in the hypothesis where only one of the two components in the kinetic energy distribution is considered to estimate the yield (blue and green dots). The disagreement of our corrected values with the JEFF-3.1.1 evaluation is still present. The mean kinetic energy for the two components and for the whole kinetic energy distribution is also shown on the right figure, after correction from the energy loss in the target using a set of reference data (orange dots) with a very thin target of $30 \mu\text{g}\cdot\text{cm}^{-2}$ without any cover.

An important result here is the apparition of two modes after effective decontamination. We remind that the modality of the fission process has already been observed for the Fermium region [6] and in the case of fast neutron induced fission [7]. In the punctual approximation of the Coulomb

repulsion, the total kinetic energy of fragments is related to the scission configuration by the following equation :

$$TKE = E_L + E_H \cong E_L \left(1 + \frac{m_L}{m_H} \right) = \frac{Z_L Z_H e^2}{4\pi\epsilon_0 d} \quad (4)$$

with m_i and Z_i the mass and nuclear charge of each fragment and d the distance between the two centers of charge of the fragments at the scission point. The results of this calculation, considering additional hypothesis such as the Unchanged Charge Density (UCD), are shown in Tab. 1 and compared to estimations from the Brosa approach [8] and from microscopic model calculations [9]. Our values for the low and high kinetic energy components are rather consistent with the theoretical predictions from the two models considered here. These results tend to prove the modality of the $^{233}\text{U}(n_{th}, f)$ fission process.

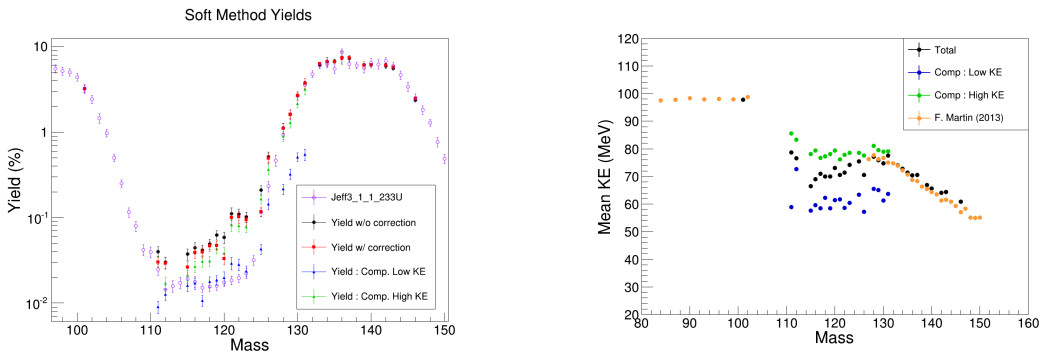


Figure 4. Mass yields per component in kinetic energy distributions compared to the Jeff-3.1.1 library (left). Mean kinetic energy of the extracted modes after energy loss corrections in the target (right).

Table 1. Comparison of scission configurations d , between our work and different fission models. Estimation of neutron emission $\bar{\nu}$ and comparison with dedicated measurement (Nishio [10]).

Component	This work	Brosa	Microscopic	Configuration	This work	Nishio
Low KE	$d \cong 24 \text{ fm}$	$d \cong 21 \text{ fm}$	$d \cong 20 \text{ fm}$	Symmetric	$\bar{\nu} \cong 7.0$	$\bar{\nu} \cong 8.0$
High KE	$d \cong 19 \text{ fm}$	$d \cong 18 \text{ fm}$	$d \cong 16 \text{ fm}$	Asymmetric	$\bar{\nu} \cong 3.6$	$\bar{\nu} \cong 4.0$

5 Conclusion and perspectives

This work presents an investigation of the $^{233}\text{U}(n_{th}, f)$ yields in the symmetry region, with a focus on the measurement of the fragment kinetic energy distributions. After a proven contamination presence and its necessary correction, two components in the distributions are observed for all of the masses around and within the symmetry but not in the high yield region.

A further study relative to possible biases in the correction process and an estimation of the uncertainties are still needed to conclude on the direct evidence of the modality of thermal neutron induced fission in the region of Uraniums. The development of a Time Of Flight setup is under development to get a triple coincidence between a double Frisch grid ionisation chamber and the velocity of the incoming fragments.

References

- [1] F. Martin *et al.*, *Proc. 2nd ANIMMA Conference*, June 2011, Ghent
- [2] F. Martin *et al.*, *Nucl. Data Sheets* **119**, 328-330 (2014)
- [3] The JEFF-3.1.1 nuclear data library, OECD, NEA, JEFF Report 21, ISBN 92-64-02314-3 (2006)
- [4] P. Armbruster *et al.*, *Nucl. Instrum. Methods* **139** 213 (1976)
- [5] R. Brissot *et al.*, *Physics and Chemistry of Fission 1979*, IAEA, 99-110 (1980)
- [6] E.K. Hulet *et al.*, *Phys. Rev. C* **40**, 770 (1989)
- [7] E. Pfeiffer *et al.*, *Z. Phys.* **240**, 403 (1970)
- [8] U. Brosa *et al.*, *Phys. Reports* **197**, 167 (1990)
- [9] H. Goutte *et al.*, *Phys. Rev. C* **71**, 024316 (2005)
- [10] K. Nishio *et al.*, *J. Nucl. Sc. Tech.* **35**, 631 (1998)